ЖЭТФ, 2012, том 142, вып. 1 (7), стр. 156–168

THE EFFECT OF COULOMB CORRELATIONS ON THE NONEQUILIBRIUM CHARGE REDISTRIBUTION TUNED BY THE TUNNELING CURRENT

P. I. Arseev[b], **N. S. Maslova**[a], **V. N. Mantsevich**[a*]

[a] *Lomonosov Moscow State University*
119991, Moscow, Russia

[b] *Lebedev Physical Institute*
119991, Moscow, Russia

Received October 7, 2011

We demonstrate that the tunneling current flowing through a system with Coulomb correlations leads to a charge redistribution between the different localized states. A simple model consisting of two electron levels is analyzed by means of the Heisenberg equations of motion taking correlations of electron filling numbers in localized states into account exactly in all orders. We consider various relations between the Coulomb interaction and localized electron energies. Sudden jumps of the electron density at each level in a certain range of the applied bias are found. We find that for some parameter range, inverse occupation in the two-level system appears due to Coulomb correlations. It is also shown that Coulomb correlations lead to the appearance of negative tunneling conductivity at a certain relation between the values of tunneling rates from the two electron levels.

1. INTRODUCTION

Nonequilibrium Coulomb correlations can drastically affect the local charge distribution in the vicinity of impurity complexes in nanometer tunneling junctions. Coulomb interaction results in significant changes of electron filling numbers in each localized state and of current–voltage (I–V) characteristics of impurity complexes. Adjusting the parameters of a tunneling contact allows obtaining negative tunneling conductivity caused by Coulomb correlations in a certain range of the applied bias. There are several experimental situations in which Coulomb interaction values are of the order of the electron level spacing or even greatly exceed it. This usually occurs if the distance between several impurity atoms or surface defects is comparable to the lattice scale, and hence the coupling between their electron states can greatly exceed the interaction of these localized states with the continuous spectrum.

Another possible realization is a quantum dot or two small interacting quantum dots on a sample surface weakly connected with bulk states. Such systems can be described by a model including several electron levels with Coulomb interaction between localized electrons. The electronic structure of such complexes can be tuned both by an external electric field that changes the values of single-particle levels and by electron correlations of localized electron states. In a nonequilibrium situation, Coulomb correlations can be expected to result in a spatial redistribution of localized charges and the possibility of local charge density manipulation governed by Coulomb correlations. In some sense, these effects are similar to the "co-tunneling" observed in [1, 2]. Moreover, Coulomb interaction of localized electrons can be responsible for the inverse occupation of localized electron states and negative local tunneling conductivity in a certain range of applied bias. These effects can be clearly seen if single-electron levels have different spatial symmetries.

The nonmonotonic filling of individual quantum dots as a function of gate voltage due to the competition between tunneling and Coulomb interaction in a system of coupled single-level quantum dots with spinless electrons was analyzed in [3]. But the authors studied only first-order correlations in the limit of a large

*E-mail: vmantsev@smplab.phys.msu.ru

value of Coulomb interaction (higher than a level spacing and level broadening) and paid attention mostly to the dependence of individual quantum dots filling numbers on temperature. A nonmonotonic charge occupation was already investigated when reservoirs coupled to quantum dots were replaced by single levels [4, 5].

Much attention has been paid to electron transport through a single impurity or a dot in the Coulomb blockade and the Kondo [6] regimes. These effects have been studied experimentally and are currently under theoretical investigation [7–13]. But if the tunneling coupling is not negligible, the impurity charge is not a discrete value and one has to deal with impurity electron filling numbers (which become continuous variables) determined from kinetic equations.

Nonequilibrium effects and tunneling current spectra in the system of two weakly coupled impurities (when the coupling between impurities is smaller than the tunneling rates between energy levels and tunneling contact leads) in the presence of Coulomb interaction were described by a self-consistent approach based on the Keldysh diagram technique in [14, 15]. In this paper, we consider the opposite case where the Coulomb coupling between localized electron states is much greater than the tunneling transfer rates.

We propose a theoretical approach based on the Heisenberg equations for localized state electron filling numbers taking local electron density correlations into account in all orders [16]. The tunneling current in a two-level system of spinless fermions with an infinite value of Coulomb interaction has been investigated in [17]. But the obtained results do not take any nontrivial pair correlations for finite Coulomb correlations into account. If we are interested in kinetic properties with the applied bias range larger than the characteristic energy of correlations between localized and band electrons in the leads, then the Kondo effect is unimportant. In this case, for a finite number of localized electron levels, a closed system of equations for electron filling numbers and all their correlators can be obtained. It allows analyzing the role of Coulomb correlations in charge redistribution and in the formation of main features of I–V characteristics.

2. THE PROPOSED MODEL

We analyze tunneling through the two-level system with Coulomb interaction of localized electrons sketched in Fig. 1. The model system can be described by the Hamiltonian

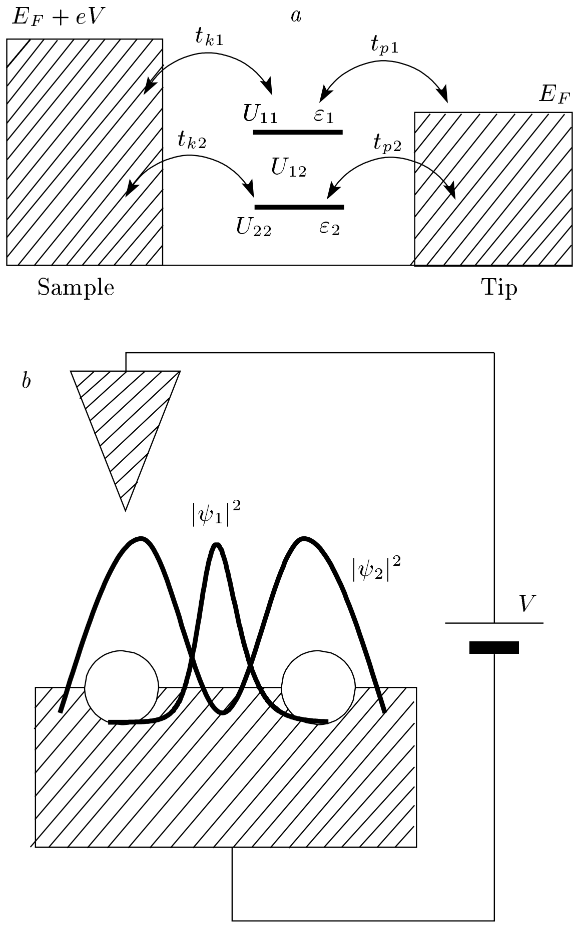

Fig. 1. Energy diagram of a two-level system (a) and schematic spatial diagram of experimental realization (b). Coulomb energy U_{ij} corresponds to the interaction between electrons on different energy levels

$$\hat{H} = \sum_{i\sigma} \varepsilon_i n_{i\sigma} + \sum_{k\sigma} \varepsilon_k c_{k\sigma}^{+} c_{k\sigma} + \\ + \sum_{p\sigma} \varepsilon_p c_{p\sigma}^{+} c_{p\sigma} + \sum_{ij\sigma\sigma'} U_{ij}^{\sigma\sigma'} n_{i\sigma} n_{j\sigma'} + \\ + \sum_{ki\sigma} t_{ki} (c_{k\sigma}^{+} c_{i\sigma} + \text{h.c.}) + \sum_{pi\sigma} t_{pi} (c_{p\sigma}^{+} c_{i\sigma} + \text{h.c.}), \quad (1)$$

where the indices k and p respectively label continuous spectrum states in the left (sample) and right (tip) leads of tunneling contact and $t_{k(p)}$ are the tunneling transfer amplitudes between continuous spectrum states and localized states with energies ε_i. The operators $c_{k(p)}^{+}/c_{k(p)}$ correspond to electron creation/annihilation in the continuous spectrum states $k(p)$ and $n_{i\sigma} = c_{i\sigma}^{+} c_{i\sigma}$ are the two-level system electron filling numbers, where the operator $c_{i\sigma}$ destroys an electron with spin σ on the energy level ε_i.

The tunneling current through the two-level system is written in terms of the electron creation/annihilation operators as

$$I = I_{k\sigma} = \sum_{i\sigma} I_{ki\sigma} = \sum_{k\sigma} \dot{n}_{k\sigma} = \sum_{ki\sigma} t_{ki}(\langle c_{k\sigma}^{+} c_{i\sigma}\rangle - \langle c_{i\sigma}^{+} c_{k\sigma}\rangle). \quad (2)$$

We set $\hbar = 1$, and therefore equations of motion for the product $c_{k\sigma}^{+} c_{i\sigma}$ of electron operators can be written as

$$i\frac{\partial c_{k\sigma}^{+} c_{i\sigma}}{\partial t} = (\varepsilon_i - \varepsilon_k) c_{k\sigma}^{+} c_{i\sigma} + U_{ii} n_{i-\sigma} c_{k\sigma}^{+} c_{i\sigma} + U_{ij}(n_{j\sigma} + n_{j-\sigma}) c_{k\sigma}^{+} c_{i\sigma} - t_{ki}(n_{i\sigma} - \widehat{f}_k) + \sum_{k' \neq k} t_{k'i} c_{k\sigma}^{+} c_{k'\sigma} + \sum_{i \neq j} t_{kj} c_{j\sigma}^{+} c_{i\sigma} = 0, \quad (3)$$

where

$$\widehat{f}_k = c_{k\sigma}^{+} c_{k\sigma}. \quad (4)$$

To obtain an equation for the tunneling current, we multiply Eq. (3) by combinations of the electron filling number operators $n_{i(j)\pm\sigma}$:

$$(1 - n_{1-\sigma})(1 - n_{2-\sigma})(1 - n_{2\sigma}) c_{k\sigma}^{+} c_{1\sigma} = \left\{ \left(t_{k1}(n_{1\sigma} - \widehat{f}_k) + \sum_{k' \neq k} t_{k'1} c_{k\sigma}^{+} c_{k'\sigma} + t_{k2} c_{2\sigma}^{+} c_{1\sigma} \right) \times (1 - n_{1-\sigma})(1 - n_{2-\sigma})(1 - n_{2\sigma}) \right\} \{\varepsilon_1 - \varepsilon_k\}^{-1}, \quad (5)$$

$$n_{1-\sigma}(1 - n_{2-\sigma})(1 - n_{2\sigma}) c_{k\sigma}^{+} c_{1\sigma} = \left\{ \left(t_{k1}(n_{1\sigma} - \widehat{f}_k) + \sum_{k' \neq k} t_{k'1} c_{k\sigma}^{+} c_{k'\sigma} + t_{k2} c_{2\sigma}^{+} c_{1\sigma} \right) \times n_{1-\sigma}(1 - n_{2-\sigma})(1 - n_{2\sigma}) \right\} \{\varepsilon_1 - \varepsilon_k + U_{11}\}^{-1}, \quad (6)$$

$$\sum_{\sigma'} n_{2\sigma'}(1 - n_{1-\sigma})(1 - n_{2-\sigma'}) c_{k\sigma}^{+} c_{1\sigma} = \sum_{\sigma'} \left\{ \left(t_{k1}(n_{1\sigma} - \widehat{f}_k) + \sum_{k' \neq k} t_{k'1} c_{k\sigma}^{+} c_{k'\sigma} + t_{k2} c_{2\sigma}^{+} c_{1\sigma} \right) \times n_{2\sigma'}(1 - n_{1-\sigma})(1 - n_{2-\sigma'}) \right\} \{\varepsilon_1 - \varepsilon_k + U_{12}\}^{-1}, \quad (7)$$

$$\sum_{\sigma'} n_{1-\sigma} n_{2\sigma'}(1 - n_{2-\sigma'}) c_{k\sigma}^{+} c_{1\sigma} = \sum_{\sigma'} \left\{ \left(t_{k1}(n_{1\sigma} - \widehat{f}_k) + \sum_{k' \neq k} t_{k'1} c_{k\sigma}^{+} c_{k'\sigma} + t_{k2} c_{2\sigma}^{+} c_{1\sigma} \right) \times n_{1-\sigma} n_{2\sigma'}(1 - n_{2-\sigma'}) \right\} \{\varepsilon_1 - \varepsilon_k + U_{11} + U_{12}\}^{-1}, \quad (8)$$

$$n_{2-\sigma} n_{2\sigma}(1 - n_{1-\sigma}) c_{k\sigma}^{+} c_{1\sigma} = \left\{ \left(t_{k1}(n_{1\sigma} - \widehat{f}_k) + \sum_{k' \neq k} t_{k'1} c_{k\sigma}^{+} c_{k'\sigma} + t_{k2} c_{2\sigma}^{+} c_{1\sigma} \right) \times n_{2-\sigma} n_{2\sigma}(1 - n_{1-\sigma}) \right\} \{\varepsilon_1 - \varepsilon_k + 2U_{12}\}^{-1}, \quad (9)$$

$$n_{1-\sigma} n_{2-\sigma} n_{2\sigma} c_{k\sigma}^{+} c_{1\sigma} = \left\{ \left(t_{k1}(n_{1\sigma} - \widehat{f}_k) + \sum_{k' \neq k} t_{k'1} c_{k\sigma}^{+} c_{k'\sigma} + t_{k2} c_{2\sigma}^{+} c_{1\sigma} \right) \times n_{1-\sigma} n_{2-\sigma} n_{2\sigma} \right\} \{\varepsilon_1 - \varepsilon_k + U_{11} + 2U_{12}\}^{-1}. \quad (10)$$

The relation $n_{i\sigma}^2 = n_{i\sigma}$ was used in these equations.

Neglecting changes in the electron spectrum and local density of states in the tunneling contact leads caused by the tunneling current, we uncouple the conduction and localized electron filling numbers. This also means that we neglect any correlation effects between localized and band electrons, similarly ħ the case of the Kondo effect.

It is easy to check verify that

$$(1 - n_{1-\sigma})(1 - n_{2-\sigma})(1 - n_{2\sigma}) + n_{1-\sigma}(1 - n_{2-\sigma})(1 - n_{2\sigma}) + \sum_{\sigma'} n_{2\sigma'}(1 - n_{1-\sigma})(1 - n_{2-\sigma'}) + \sum_{\sigma'} n_{1-\sigma} n_{2\sigma'}(1 - n_{2-\sigma'}) + n_{2-\sigma} n_{2\sigma}(1 - n_{1-\sigma}) + n_{1-\sigma} n_{2-\sigma} n_{2\sigma} = 1. \quad (11)$$

Adding the right- and left-hand sides of Eqs. (5)–(10), we then obtain an equation for $\langle c_{k\sigma}^{+} c_{i\sigma}\rangle$, which after a summation over k yields an equation for the tunneling current through the two-level system. The total current is the sum of two contributions,

$$I_{k\sigma} = I_{k1\sigma} + I_{k2\sigma}, \quad (12)$$

where the expression for the tunneling current $I_{k2\sigma}$ can be obtained by changing indexes $1 \leftrightarrow 2$ in the equation for the tunneling current $I_{k1\sigma}$, which is given by

$$\begin{aligned} I_{k1\sigma} = \Gamma_{k1}\{\langle n_{1\sigma}\rangle - \langle(1-n_{1-\sigma})(1-n_{2-\sigma})(1-n_{2\sigma})\rangle \times \\ \times f_k(\varepsilon_1) - \langle n_{1-\sigma}(1-n_{2-\sigma})(1-n_{2\sigma})\rangle f_k(\varepsilon_1+U_{11}) - \\ - \langle n_{2\sigma}(1-n_{2-\sigma})(1-n_{1-\sigma})\rangle f_k(\varepsilon_1+U_{12}) - \\ - \langle n_{2-\sigma}(1-n_{2\sigma})(1-n_{1-\sigma})\rangle f_k(\varepsilon_1+U_{12}) - \\ - \langle n_{1-\sigma}n_{2\sigma}(1-n_{2-\sigma})\rangle f_k(\varepsilon_1+U_{11}+U_{12}) - \\ - \langle n_{1-\sigma}n_{2-\sigma}(1-n_{2\sigma})\rangle f_k(\varepsilon_1+U_{11}+U_{12}) - \\ - \langle n_{2\sigma}n_{2-\sigma}(1-n_{1-\sigma})\rangle f_k(\varepsilon_1+2U_{12}) - \\ - \langle n_{1-\sigma}n_{2-\sigma}n_{2\sigma}\rangle f_k(\varepsilon_1+U_{11}+2U_{12})\} + \\ + t_{k1}t_{k2}\nu_{0k}c^+_{2\sigma}c_{1\sigma} + \sum_{k'\neq k}\langle t_{k1}t_{k'1}c^+_{k\sigma}c_{k'\sigma}\rangle \times \\ \times \left\{\left\langle\frac{(1-n_{1-\sigma})(1-n_{2-\sigma})(1-n_{2\sigma})}{\varepsilon_1-\varepsilon_k}\right\rangle + \right. \\ + \left\langle\frac{n_{1-\sigma}(1-n_{2-\sigma})(1-n_{2\sigma})}{\varepsilon_1+U_{11}-\varepsilon_k}\right\rangle + \\ + \left\langle\frac{\sum_{\sigma'} n_{2\sigma'}(1-n_{1-\sigma})(1-n_{2-\sigma'})}{\varepsilon_1+U_{12}-\varepsilon_k}\right\rangle + \\ + \left\langle\frac{\sum_{\sigma'} n_{1-\sigma}n_{2\sigma'}(1-n_{2-\sigma'})}{\varepsilon_1+U_{11}+U_{12}-\varepsilon_k}\right\rangle + \\ + \left\langle\frac{n_{2-\sigma}n_{2\sigma}(1-n_{1-\sigma})}{\varepsilon_1+2U_{12}-\varepsilon_k}\right\rangle + \\ \left. + \left\langle\frac{n_{1-\sigma}n_{2-\sigma}n_{2\sigma}}{\varepsilon_1+U_{11}+2U_{12}-\varepsilon_k}\right\rangle\right\}. \end{aligned} \quad (13)$$

In what follows, we neglect the terms $t_{k1}t_{k2}\nu_{0k}c^+_{2\sigma}c_{1\sigma}$ and terms proportional to $t_{k1}t_{k'1}c^+_{k\sigma}c_{k'\sigma}/(\varepsilon_1-\varepsilon_k)$ in expression (13) because they correspond to the next-order perturbation theory in the parameter Γ_i/ε_i. The relaxation rates

$$\Gamma_{k(p)i} = \pi t^2_{k(p)i}\nu_0$$

are determined by electron tunneling transitions from the two-level system to the leads k (sample) and p (tip) continuum states; $\nu_{0k(p)}$ is the continuous spectrum density of states. The main equation for the current (13) includes mean electron filling numbers $n_{i\sigma}$ and pair and triple correlators for the localized states, which have to be determined. Equations for the total electron filling numbers $n_{1\sigma}$ and $n_{2\sigma}$ on levels 1 and 2 can be found from the conditions

$$\begin{aligned} \frac{\partial n_{1\sigma}}{\partial t} = I_{k1\sigma} + I_{p1\sigma} = 0, \\ \frac{\partial n_{2\sigma}}{\partial t} = I_{k2\sigma} + I_{p2\sigma} = 0, \end{aligned} \quad (14)$$

where the tunneling current $I_{p\sigma}$ can be easily obtained from $I_{k\sigma}$ by changing indexes $k \leftrightarrow p$. Pair filling number correlators can be found as

$$\left\langle\frac{\partial n_{i\sigma}n_{j\sigma'}}{\partial t}\right\rangle = \left\langle\frac{\partial n_{i\sigma}}{\partial t}n_{j\sigma'}\right\rangle + \left\langle\frac{\partial n_{j\sigma'}}{\partial t}n_{i\sigma}\right\rangle. \quad (15)$$

The full expressions that determine the system of equations for pair filling number correlators in terms of higher-order correlators in the stationary case are

$$\begin{aligned} \left\langle\frac{\partial n_{i\sigma}n_{j\sigma'}}{\partial t}\right\rangle = (\Gamma_{ki}+\Gamma_{pi}+\Gamma_{kj}+\Gamma_{pj}) \times \\ \times \langle n_{i\sigma}n_{j\sigma'}\rangle - (\Gamma_{ki}f_k(\varepsilon_i+U_{ij}) + \Gamma_{pi}f_p(\varepsilon_i+U_{ij})) \times \\ \times \langle n_{j\sigma'}(1-n_{j-\sigma'})(1-n_{i-\sigma})\rangle - \\ - (\Gamma_{kj}f_k(\varepsilon_j+U_{ij}) + \Gamma_{pj}f_p(\varepsilon_j+U_{ij})) \times \\ \times \langle n_{i\sigma}(1-n_{i-\sigma})(1-n_{j-\sigma'})\rangle - \\ - (\Gamma_{ki}f_k(\varepsilon_i+U_{ii}+U_{ij}) + \Gamma_{pi}f_p(\varepsilon_i+U_{ii}+U_{ij})) \times \\ \times \langle n_{i-\sigma}n_{j\sigma'}(1-n_{j-\sigma'})\rangle - \\ - (\Gamma_{ki}f_k(\varepsilon_i+2U_{ij}) + \Gamma_{pi}f_p(\varepsilon_i+2U_{ij})) \times \\ \times \langle n_{j-\sigma'}n_{j\sigma'}(1-n_{i-\sigma})\rangle - \\ - (\Gamma_{ki}f_k(\varepsilon_i+U_{ii}+2U_{ij}) + \Gamma_{pi}f_p(\varepsilon_i+U_{ii}+2U_{ij})) \times \\ \times \langle n_{i-\sigma}n_{j\sigma'}n_{j-\sigma'}\rangle - \\ - (\Gamma_{kj}f_k(\varepsilon_j+U_{jj}+U_{ij}) + \Gamma_{pj}f_p(\varepsilon_j+U_{jj}+U_{ij})) \times \\ \times \langle n_{j-\sigma'}n_{i\sigma}(1-n_{i-\sigma})\rangle - \\ - (\Gamma_{kj}f_k(\varepsilon_j+2U_{ij}) + \Gamma_{pj}f_p(\varepsilon_j+2U_{ij})) \times \\ \times \langle n_{i-\sigma}n_{j\sigma'}(1-n_{j-\sigma'})\rangle - \\ - (\Gamma_{kj}f_k(\varepsilon_j+U_{jj}+2U_{ij}) + \Gamma_{pj}f_p(\varepsilon_j+U_{jj}+2U_{ij})) \times \\ \times \langle n_{j-\sigma'}n_{i\sigma}n_{i-\sigma}\rangle\} = 0. \end{aligned} \quad (16)$$

Higher-order correlators can be found similarly:

$$\begin{aligned} \left\langle\frac{\partial n_{j\sigma}n_{j-\sigma}n_{i-\sigma'}}{\partial t}\right\rangle = \left\langle\frac{\partial n_{j\sigma}n_{j-\sigma}}{\partial t}n_{i-\sigma'}\right\rangle + \\ + \left\langle\frac{\partial n_{i-\sigma'}}{\partial t}n_{j\sigma}n_{j-\sigma}\right\rangle. \end{aligned} \quad (17)$$

Hence, the higher-order correlators are given by

$$\begin{aligned} \langle n_{j\sigma}n_{j-\sigma}n_{i-\sigma'}\rangle = \{\Gamma_{kj}f_k(\varepsilon_j+U_{jj}+2U_{ij}) \times \\ \times (\langle n_{i-\sigma}n_{j\sigma}\rangle + \langle n_{i-\sigma}n_{j-\sigma}\rangle) + \\ + \Gamma_{ki}f_k(\varepsilon_i+2U_{ij})\langle n_{j\sigma}n_{j-\sigma}\rangle + \\ + \Gamma_{pj}f_p(\varepsilon_j+U_{jj}+2U_{ij}) \times \\ \times (\langle n_{i-\sigma}n_{j\sigma}\rangle + \langle n_{i-\sigma}n_{j-\sigma}\rangle) + \\ + \Gamma_{pi}f_p(\varepsilon_i+2U_{ij})\langle n_{j\sigma}n_{j-\sigma}\rangle\} \times \\ \times \{\Gamma_{ki}\{3+f_k(\varepsilon_i+2U_{ij})-f_k(\varepsilon_i+U_{ii}+2U_{ij})\} + \\ + \Gamma_{pi}\{3+f_p(\varepsilon_i+2U_{ij})-f_p(\varepsilon_i+U_{ii}+2U_{ij})\}\}^{-1}. \end{aligned} \quad (18)$$

We consider the paramagnetic situation

$$n_{i\sigma} = n_{i-\sigma}, \quad \langle n_{i\sigma} n_{j\sigma}\rangle = \langle n_{i\sigma} n_{j-\sigma}\rangle,$$

$$\langle n_{i\sigma} n_{i-\sigma} n_{j\sigma}\rangle = \langle n_{i\sigma} n_{i-\sigma} n_{j-\sigma}\rangle.$$

(We note that system of equations (14)–(19) also allows analyzing the magnetic regime with $n_{i\sigma} \neq n_{i-\sigma}$.) After the substitution of Eq. (18) in (16), the system of equations for the pair correlators

$$K_{11} \equiv \langle n_{1\sigma} n_{1-\sigma}\rangle, \quad K_{22} \equiv \langle n_{2\sigma} n_{2-\sigma}\rangle,$$

$$K_{12} \equiv \langle n_{1\sigma} n_{2\sigma}\rangle$$

becomes

$$\begin{pmatrix} a_{11} & a_{12} & a_{13} \\ a_{21} & a_{22} & a_{23} \\ a_{31} & a_{32} & a_{33} \end{pmatrix} \times \begin{pmatrix} K_{11} \\ K_{12} \\ K_{22} \end{pmatrix} = F \tag{19}$$

with the coefficients

$$\begin{gathered} a_{11} = 1, \\ a_{12} = 2n_1^T(\varepsilon_1 + U_{11}) - n_1^T(\varepsilon_1 + U_{11} + U_{12}) - \\ - 2\frac{\Gamma_2}{\Gamma_1} n_2^T(\varepsilon_2 + U_{22} + U_{12})\Phi_1, \\ a_{13} = -n_1^T(\varepsilon_1 + 2U_{12})\Phi_1, \end{gathered} \tag{20}$$

$$\begin{gathered} a_{21} = -n_2^T(\varepsilon_2 + 2U_{12})\Phi_2, \\ a_{22} = 2n_2^T(\varepsilon_2 + U_{22}) - n_2^T(\varepsilon_2 + U_{22} + U_{12}) - \\ -2\frac{\Gamma_1}{\Gamma_2} n_1^T(\varepsilon_1 + U_{11} + U_{12})\Phi_2, \\ a_{23} = 1, \end{gathered} \tag{21}$$

$$\begin{gathered} a_{31} = \frac{\Gamma_2}{\Gamma_1 + \Gamma_2}(n_2^T(\varepsilon_2 + U_{12}) - \\ - n_2^T(\varepsilon_2 + 2U_{12})(1 + 2A_2)), \\ a_{32} = 1 + \frac{\Gamma_1}{\Gamma_1 + \Gamma_2}(n_1^T(\varepsilon_1 + U_{12}) - \\ - n_1^T(\varepsilon_1 + U_{11} + U_{12})(1 + 4A_2)) + \\ + \frac{\Gamma_2}{\Gamma_1 + \Gamma_2}(n_2^T(\varepsilon_2 + U_{12}) - \\ - n_2^T(\varepsilon_2 + U_2 + U_{12})(1 + 4A_1)), \\ a_{33} = \frac{\Gamma_1}{\Gamma_1 + \Gamma_2}(n_1^T(\varepsilon_1 + U_{12}) - \\ - n_1^T(\varepsilon_1 + 2U_{12})(1 + 2A_1)), \end{gathered} \tag{22}$$

where $\Gamma_i = \Gamma_{ki} + \Gamma_{pi}$ and we introduced tunneling filling numbers $n_i^T(\varepsilon_i)$ and $n_i^T(\varepsilon_i + U_{ij})$ in the absence of Coulomb interaction:

$$n_i^T(\varepsilon) = \frac{\Gamma_{ki} f_k(\varepsilon) + \Gamma_{pi} f_p(\varepsilon)}{\Gamma_{ki} + \Gamma_{pi}}. \tag{23}$$

The coefficients Φ_i and A_i can then be found as

$$\begin{gathered} \Phi_i = \frac{n_i^T(\varepsilon_i + U_{ii}) - n_i^T(\varepsilon_i + U_{ii} + U_{ij})}{3 + n_i^T(\varepsilon_i + 2U_{ij}) - n_i^T(\varepsilon_i + U_{ii} + 2U_{ij})} + \frac{n_i^T(\varepsilon_i + U_{ii} + 2U_{ij})}{3 + n_i^T(\varepsilon_i + 2U_{ij}) - n_i^T(\varepsilon_i + U_{ii} + 2U_{ij})}, \\ A_i = \frac{(1/2)n_i^T(\varepsilon_i + U_{ij}) - (1/2)n_i^T(\varepsilon_i + U_{ii} + U_{ij})}{3 + n_i^T(\varepsilon_i + 2U_{ij}) - n_i^T(\varepsilon_i + U_{ii} + 2U_{ij})} - \frac{(1/2)n_i^T(\varepsilon_i + 2U_{ij}) + (1/2)n_i^T(\varepsilon_i + U_{ii} + 2U_{ij})}{3 + n_i^T(\varepsilon_i + 2U_{ij}) - n_i^T(\varepsilon_i + U_{ii} + 2U_{ij})}, \end{gathered} \tag{24}$$

$$F = \begin{pmatrix} n_1^T(\varepsilon_1 + U_{11}) n_{1\sigma} \\ n_2^T(\varepsilon_2 + U_{22}) n_{2\sigma} \\ \frac{\Gamma_1}{\Gamma_1 + \Gamma_2} n_1^T(\varepsilon_1 + U_{12}) n_{2\sigma} + \frac{\Gamma_2}{\Gamma_1 + \Gamma_2} n_2^T(\varepsilon_2 + U_{12}) n_{1\sigma} \end{pmatrix}. \tag{25}$$

Pair correlators K_{ij} can be expressed through $n_{i(j)}$ using Eqs. (19)–(25). Substituting the solution for higher-order correlators obtained from Eqs. (16) and (18) in Eq. (14), we can find $\langle n_{i\sigma}\rangle$ and finally the tunneling current.

For large U_{ij}, we retain only states with at most two electrons in the quantum dot (neglecting triple correlators). Then the expressions for the tunneling current and the pair correlators K_{ij} become

$$\begin{aligned} I_{k1\sigma} = \Gamma_k\{\langle n_{1\sigma}\rangle - (1 - \langle n_{1\sigma}\rangle - 2\langle n_{2\sigma}\rangle + K_{22} + 2K_{12}) f_k(\varepsilon_1) - (\langle n_{1\sigma}\rangle - 2K_{12}) f_k(\varepsilon_1 + U_{11}) - \\ - 2(\langle n_{2\sigma}\rangle - K_{12} - K_{22}) f_k(\varepsilon_1 + U_{12}), \end{aligned} \tag{26}$$

$$K_{12} = \frac{(1/2)n^T(\varepsilon_1 + U_{12})(1 - n^T(\varepsilon_2 + U_{22}))n_{2\sigma} + (1/2)n^T(\varepsilon_2 + U_{12})(1 - n^T(\varepsilon_1 + U_{11}))n_{1\sigma}}{1 + n^T(\varepsilon_1 + U_{12})((1/2) - n^T(\varepsilon_2 + U_{22})) + n^T(\varepsilon_2 + U_{12})((1/2) - n^T(\varepsilon_1 + U_{11}))}, \tag{27}$$

$$K_{11} = \frac{(1+(1/2)n^T(\varepsilon_1+U_{12}) - (1/2)n^T(\varepsilon_2+U_{12}) - n^T(\varepsilon_1+U_{12})n^T(\varepsilon_2+U_{22}))n^T(\varepsilon_1+U_{11})n_{1\sigma}}{1+n^T(\varepsilon_1+U_{12})((1/2)-n^T(\varepsilon_2+U_{22}))+n^T(\varepsilon_2+U_{12})((1/2)-n^T(\varepsilon_1+U_{11}))} - \\ - \frac{n^T(\varepsilon_1+U_{11})n^T(\varepsilon_1+U_{12})(1-n^T(\varepsilon_2+U_{22}))n_{2\sigma}}{1+n^T(\varepsilon_1+U_{12})((1/2)-n^T(\varepsilon_2+U_{22}))+n^T(\varepsilon_2+U_{12})((1/2)-n^T(\varepsilon_1+U_{11}))}, \quad (28)$$

$$K_{22} = \frac{(1+(1/2)n^T(\varepsilon_2+U_{12}) - (1/2)n^T(\varepsilon_1+U_{12}) - n^T(\varepsilon_2+U_{12})n^T(\varepsilon_1+U_{11}))n^T(\varepsilon_2+U_{22})n_{2\sigma}}{1+n^T(\varepsilon_1+U_{12})((1/2)-n^T(\varepsilon_2+U_{22}))+n^T(\varepsilon_2+U_{12})((1/2)-n^T(\varepsilon_1+U_{11}))} - \\ - \frac{n^T(\varepsilon_2+U_{22})n^T(\varepsilon_2+U_{12})(1-n^T(\varepsilon_1+U_{11}))n_{1\sigma}}{1+n^T(\varepsilon_1+U_{12})((1/2)-n^T(\varepsilon_2+U_{22}))+n^T(\varepsilon_2+U_{12})((1/2)-n^T(\varepsilon_1+U_{11}))}. \quad (29)$$

When all Coulomb interaction energies are extremely large, $U_{ij} \to \infty$ or $eV \ll \varepsilon_i + U_{ij}$, expressions for the electron filling numbers n_j and the tunneling current for low temperatures have a very simple form:

$$n_{1\sigma} = \frac{n_1^T(\varepsilon_1)(1-n_2^T(\varepsilon_2))}{(1+n_1^T(\varepsilon_1))(1+n_2^T(\varepsilon_2)) - 4n_1^T(\varepsilon_1)n_2^T(\varepsilon_2)}, \\ n_{2\sigma} = \frac{n_2^T(\varepsilon_2)(1-n_1^T(\varepsilon_1))}{(1+n_1^T(\varepsilon_1))(1+n_2^T(\varepsilon_2)) - 4n_1^T(\varepsilon_1)n_2^T(\varepsilon_2)}. \quad (30)$$

The tunneling current is obtained from (26) by omitting all correlators K and terms with $f_k(\varepsilon_i + U_{ij})$:

$$I_k = \frac{4\Gamma_k\Gamma_p}{\Gamma_k+\Gamma_p} \frac{(f_p(\varepsilon_1)-f_k(\varepsilon_1))(1-n_2^T(\varepsilon_2)) + (f_p(\varepsilon_2)-f_k(\varepsilon_2))(1-n_1^T(\varepsilon_1))}{(1+n_1^T(\varepsilon_1))(1+n_2^T(\varepsilon_2)) - 4n_1^T(\varepsilon_1)n_2^T(\varepsilon_2)}. \quad (31)$$

The determinant of system (19) can vanish or even become negative for some choice of the parameters, and therefore the electron filling numbers of the two-level system can take negative values at some ranges of the applied bias voltage. Such invalid system behavior is the result of our approximation because we neglected the interaction between the two localized electron states due to the electron transitions to the continuous spectrum states in the leads and back. To improve the results, it is necessary to include the corrections that can be found using the next-order perturbation theory in the parameter Γ_i/ε_i, retaining the terms $t_{k1}t_{k2}\nu_{0k}c_{2\sigma}^+c_{1\sigma}$ in Eq. (3). In this case the final equations for $n_{i\sigma}$ have additional nonlinear terms and can be schematically written as

$$n_{1\sigma}(A_{11}+\mu_1 n_{2\sigma}^2) + n_{2\sigma}(A_{12}+\mu_2 n_{1\sigma}^2) = n^T(\varepsilon_1), \\ n_{2\sigma}(A_{22}+\nu_2 n_{1\sigma}^2) + n_{1\sigma}(A_{21}+\nu_1 n_{2\sigma}^2) = n^T(\varepsilon_2). \quad (32)$$

The coefficients A_{ij}, μ_i, and ν_i have a rather simple but cumbersome form and depend only on the tunneling filling numbers and parameters of the tunneling contact. We do not consider this case here.

3. MAIN RESULTS AND DISCUSSION

The behavior of $n_{i\sigma}$ and I–V characteristics strongly depends on the parameters of the tunneling system: energy level positions, the difference of Coulomb interaction between various localized states, and the relation between tunneling rates. The general features of all dependences are a multiple charge redistribution in the system with changing the applied bias and step-like I–V characteristics with nonequidistant steps related to the energies of various multielectron states in the quantum dots. Besides, inverse occupation of quantum dots levels and negative tunneling conductivity appear for a particular range of the system parameters and bias voltage.

We first analyze the situation where tunneling rates from both localized states to the leads are approximately equal, $t_{k(p)1} = t_{k(p)2}$. Figures 2–7 demonstrate the behavior of filling numbers and tunneling current obtained from kinetic equations for different values of the Coulomb energies U_{ij} and various electron level locations relative to the sample Fermi level in symmetric, $\Gamma_{ki} \sim \Gamma_{pi}$, and asymmetric, $\Gamma_{ki} \ll \Gamma_{pi}$ ($\Gamma_{ki} \gg \Gamma_{pi}$), tunneling contacts taking all-order correlators into account. The bias voltage in our calculations is applied to the sample. Therefore, if both levels are above (below) the Fermi level, all the specific features of charge distribution and tunneling current characteristics can be observed at negative (positive) values of eV.

In the case of both energy levels situated above (Fig. 2, Fig. 5) or below (Fig. 3, Fig. 6) the sample Fermi level, we observe the charge redistribution between electron levels of a reentrant character. When the applied bias increases, two possibilities for charge accumulation for large Coulomb energies U_{ij} are realized in turn. Charge can be localized on both electron levels equally, $n_1 = n_2$, or mostly accumulated on the lower energy level ($n_1 < n_2$). Figure 3 shows two ranges of applied bias where the upper level becomes empty, $n_1 = 0$ ($\varepsilon_2 < eV < \varepsilon_1$ and $\varepsilon_2 + U_{12} < eV < \varepsilon_1 + U_{12}$), for large values of the Coulomb energies. Decreasing the Coulomb energies leads to the situation where charge is mostly accumulated on the lower energy level (Fig. 6*c*), but $n_1 \neq 0$. In the particular range of applied bias $\varepsilon_2 < eV < \varepsilon_1 + U_{12}$, the charge is completely localized on the lower energy level: $n_1 = 0$.

Taking all-order correlators into account allows investigating tunneling through the two-level system in the case of small Coulomb energies $U_{ij} \sim \varepsilon_{i(j)}$. Figure 5 demonstrates how filling numbers and tunneling current dependences change due to a decrease in the Coulomb energies for a symmetric tunneling contact, $\Gamma_{ki} = \Gamma_{pi}$ (asymmetric contacts show the same tendencies). We demonstrate the case of both electron levels localized above the sample Fermi level.

If the Coulomb interaction is of the order of single-electron energies, three ranges of the applied bias appear where inverse occupation occurs: $n_1 > n_2$ (Fig. 5*b*) ($\varepsilon_2 + 2U_{12} < eV < \varepsilon_1 + U_{11}$, $\varepsilon_1 + 2U_{12} < eV < \varepsilon_1 + U_{11} + U_{12}$, and $\varepsilon_1 + U_{11} + 2U_{12} < eV < \varepsilon_2 + U_{22} + 2U_{12}$). Such a situation exists due to the condition that the system configuration with two electrons on the upper level and one electron on the lower level has a lower energy than the configuration with one electron on the upper level and two electrons on the lower level for the parameters shown in Fig. 5*b*. Further decreasing the Coulomb energies (Fig. 5*c*) reduces the inverse occupation effect and finally local charge mostly accumulates on the lower energy level, as it should.

We obtain that the effects of reentrant charge redistribution is more pronounced for an asymmetric contact if tunneling rates to the sample are larger than tunneling rates to the tip.

It is necessary to mention that without Coulomb interaction, filling numbers for both electron levels are simple step functions, which correspond to the tunneling filling numbers $n^T(\varepsilon_i)$ shifted from each other by the value $\varepsilon_1 - \varepsilon_2$.

The effect of inverse occupation due to Coulomb correlations is more pronounced in a system with electron levels positioned on the opposite sides of the sample Fermi level (Figs. 4 and 7). Without the Coulomb interaction, when $\Gamma_{k(p)1} = \Gamma_{k(p)2}$, the difference of the two level occupation numbers,

$$n_1 - n_2 \sim \Gamma_{k1}\Gamma_{p2} - \Gamma_{p1}\Gamma_{k2},$$

vanishes. Taking Coulomb correlations of localized electrons into account in the two-level system results in the inverse occupation of the two levels in a wide range of applied bias voltage (Figs. 4 and 7).

In Fig. 4*a,b*, we show three applied bias ranges where the inverse occupation occurs ($\varepsilon_1 + U_{11} < eV < \varepsilon_2 + 2U_{12}$, $\varepsilon_1 + 2U_{12} < eV < \varepsilon_2 + U_{22} + U_{12}$, and $\varepsilon_1 + U_{11} + U_{12} < eV$). It is evident (Fig. 3*a,b*) that when the applied bias does not exceed the value $\varepsilon_1 + U_{12}$, the entire charge is localized on the lower energy level ($n_1 = 0$). As the applied bias increases, the inverse occupation occurs and the localized charge redistributes. The inverse occupation effect strongly depends on the relation between tunneling rates. It is most pronounced in an asymmetric contact with a stronger tunneling coupling to the lead k (sample). But we have not found the inverse occupation if the two-level system is strongly coupled to the tunneling contact lead p (tip) (Fig. 4*c*). In this case, as the applied bias increases, the upper electron level charge increases but local charge is still mostly accumulated on the lower electron level.

Decreasing the Coulomb energies results in the disappearance of the inverse occupation (Fig. 7*b,c*) and local charge mostly accumulates on the lower energy level. This clearly demonstrates the role of Coulomb interaction in the charge distribution effects described here.

The tunneling current is depicted in (Figs. 2–7*d–f*) as a function of the applied bias voltage for different level positions (tunneling current amplitudes are normalized to $2\Gamma_k$). For all values of the system parameters, the tunneling current dependence on applied bias has a step-like structure. The height and length of the steps depend on the parameters of the tunneling contact (tunneling transfer rates and the values of Coulomb energies). If both levels are located below the Fermi level (Figs. 3 and 6*d–f*), the upper electron level does not appear as a step in the I–V characteristics but charge redistribution occurs due to Coulomb correlations.

For approximately equal tunneling rates for both localized levels, the I–V characteristics are mostly monotonic functions. But some new peculiarities appear if the tunneling rates are essentially different. In Fig. 8 and 9, we show some results for $t_{k(p)1} \neq t_{k(p)2}$. In this

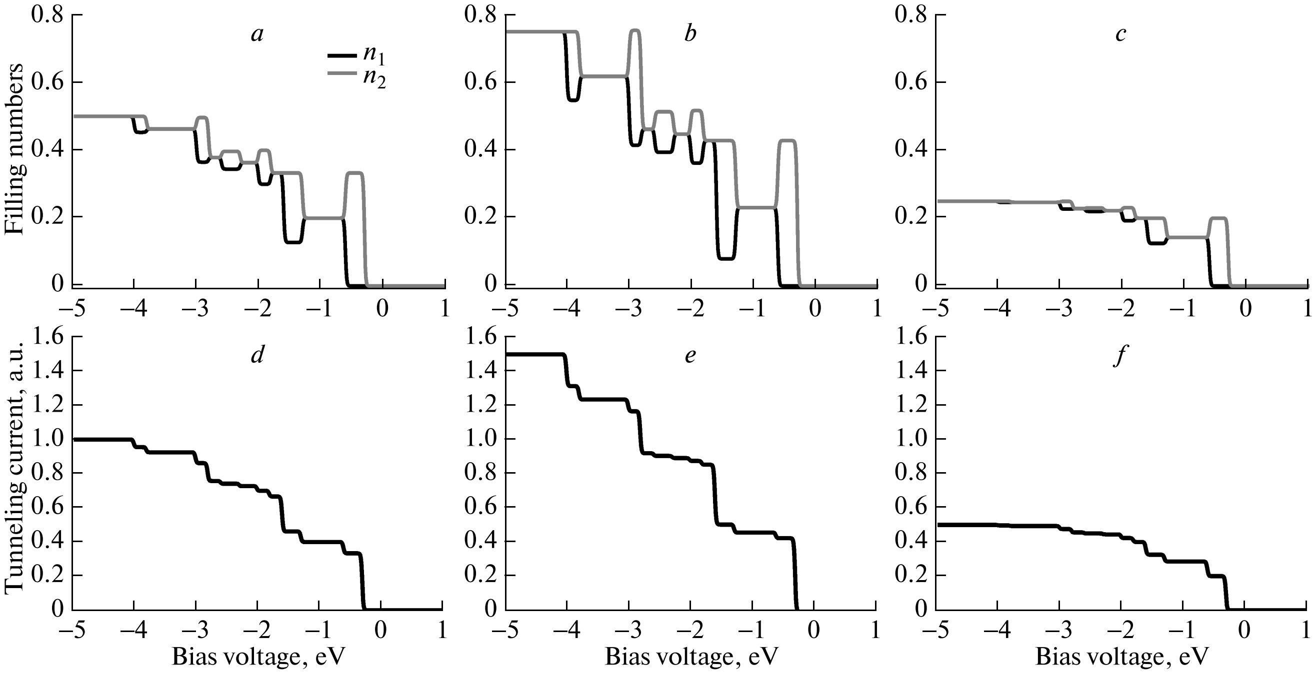

Fig. 2. Two-level system filling numbers (a–c) and tunneling current (d–f) as functions of the applied bias voltage in the case where both energy levels are located above the sample Fermi level. The parameters $\epsilon_1 = 0.6$, $\epsilon_2 = 0.3$, $U_{12} = 1.0$, $U_{11} = 1.4$, $U_{22} = 1.5$ are the same for all figures; $\Gamma_{k1} = \Gamma_{k2} = 0.01$, $\Gamma_{p1} = \Gamma_{p2} = 0.01$ (a,d); $\Gamma_{k1} = \Gamma_{k2} = 0.03$, $\Gamma_{p1} = \Gamma_{p2} = 0.01$ (b,e); $\Gamma_{k1} = \Gamma_{k2} = 0.01$, $\Gamma_{p1} = \Gamma_{p2} = 0.03$ (c,f)

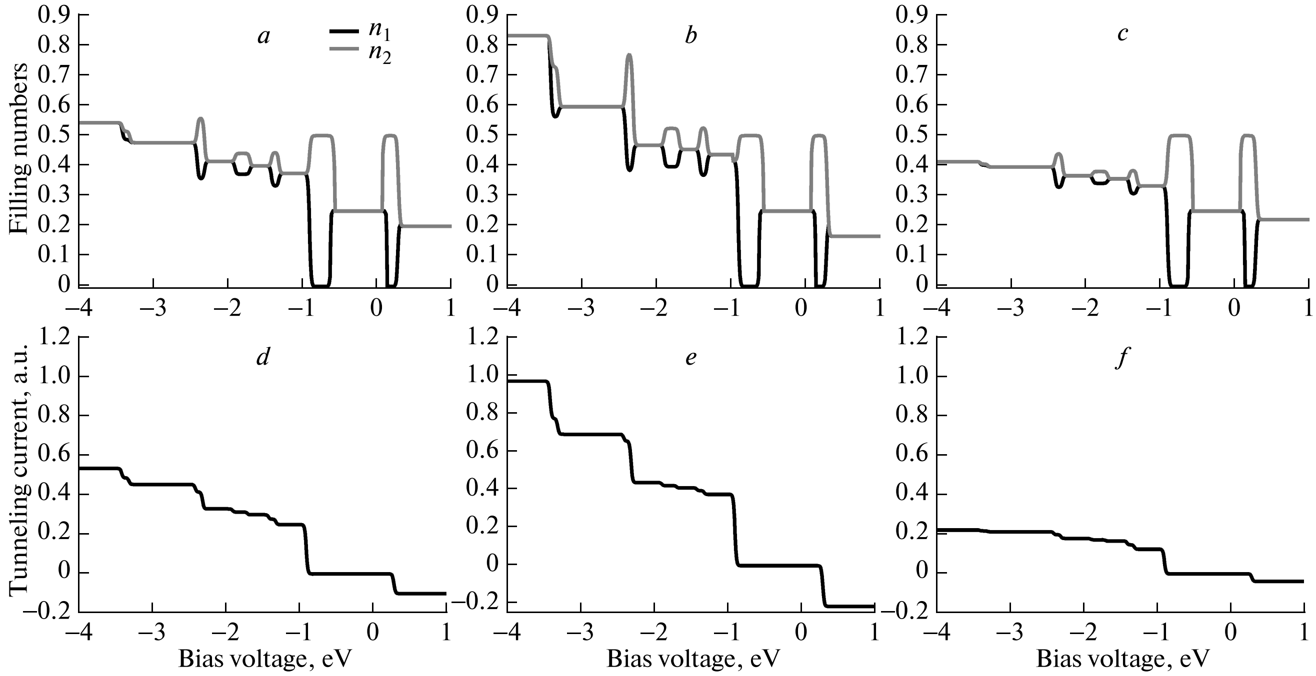

Fig. 3. Two-level system filling numbers (a–c) and tunneling current (d–f) as functions of the applied bias voltage in the case where both energy levels are located below the sample Fermi level. The parameters $\epsilon_1 = -0.1$, $\epsilon_2 = -0.3$, $U_{12} = 1.0$, $U_{11} = 1.5$, $U_{22} = 1.6$ are the same for all figures; $\Gamma_{k1} = \Gamma_{k2} = 0.01$, $\Gamma_{p1} = \Gamma_{p2} = 0.01$ (a,d); $\Gamma_{k1} = \Gamma_{k2} = 0.03$, $\Gamma_{p1} = \Gamma_{p2} = 0.01$ (b,e); $\Gamma_{k1} = \Gamma_{k2} = 0.01$, $\Gamma_{p1} = \Gamma_{p2} = 0.03$ (c,f)

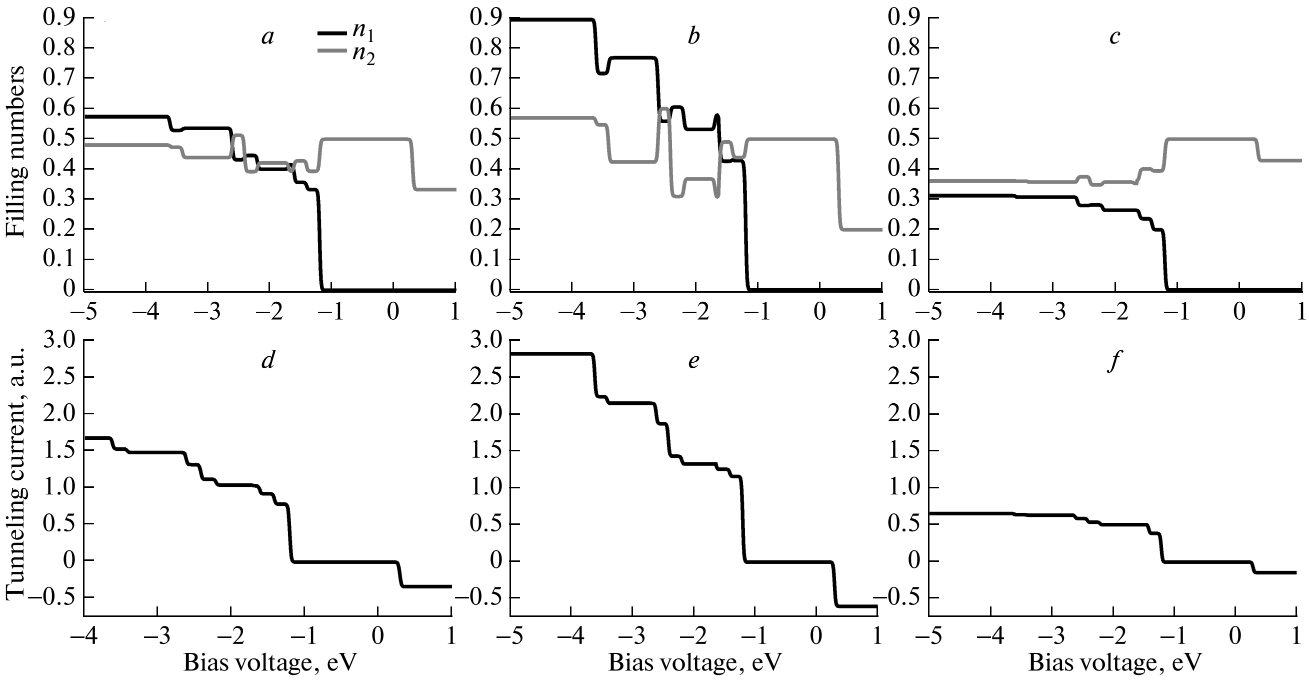

Fig. 4. Two-level system filling numbers (a–c) and tunneling current (d–f) as functions of the applied bias voltage in the case where one energy level is located above and the other — below the sample Fermi level. The parameters $\epsilon_1 = 0.2$, $\epsilon_2 = -0.3$, $U_{12} = 1.0$, $U_{11} = 1.4$, $U_{22} = 1.7$ are the same for all the figures; $\Gamma_{k1} = \Gamma_{k2} = 0.01$, $\Gamma_{p1} = \Gamma_{p2} = 0.01$ (a,d); $\Gamma_{k1} = \Gamma_{k2} = 0.03$, $\Gamma_{p1} = \Gamma_{p2} = 0.01$ (b,e); $\Gamma_{k1} = \Gamma_{k2} = 0.01$, $\Gamma_{p1} = \Gamma_{p2} = 0.03$ (c,f)

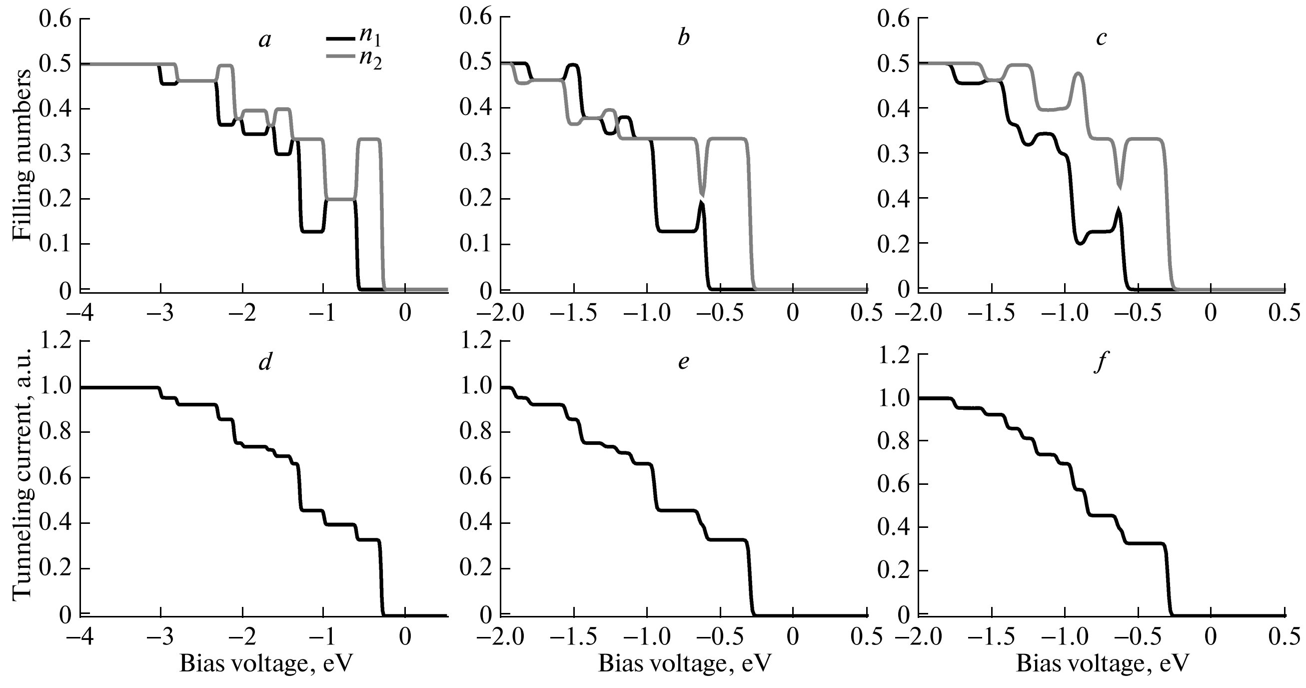

Fig. 5. Two-level system filling numbers (a–c) and tunneling current (d–f) as functions of the applied bias voltage in the case where both energy levels are located above the sample Fermi level. The parameters $\epsilon_1 = 0.6$, $\epsilon_2 = 0.3$, $\Gamma_{k1} = \Gamma_{k2} = 0.01$, $\Gamma_{p1} = \Gamma_{p2} = 0.01$ are the same for all the figures; $U_{12} = 0.7$, $U_{11} = 1.0$, $U_{22} = 1.1$ (a,d); $U_{12} = 0.35$, $U_{11} = 0.5$, $U_{22} = 0.9$ (b,e); $U_{12} = 0.35$, $U_{11} = 0.45$, $U_{22} = 0.55$ (c,f)

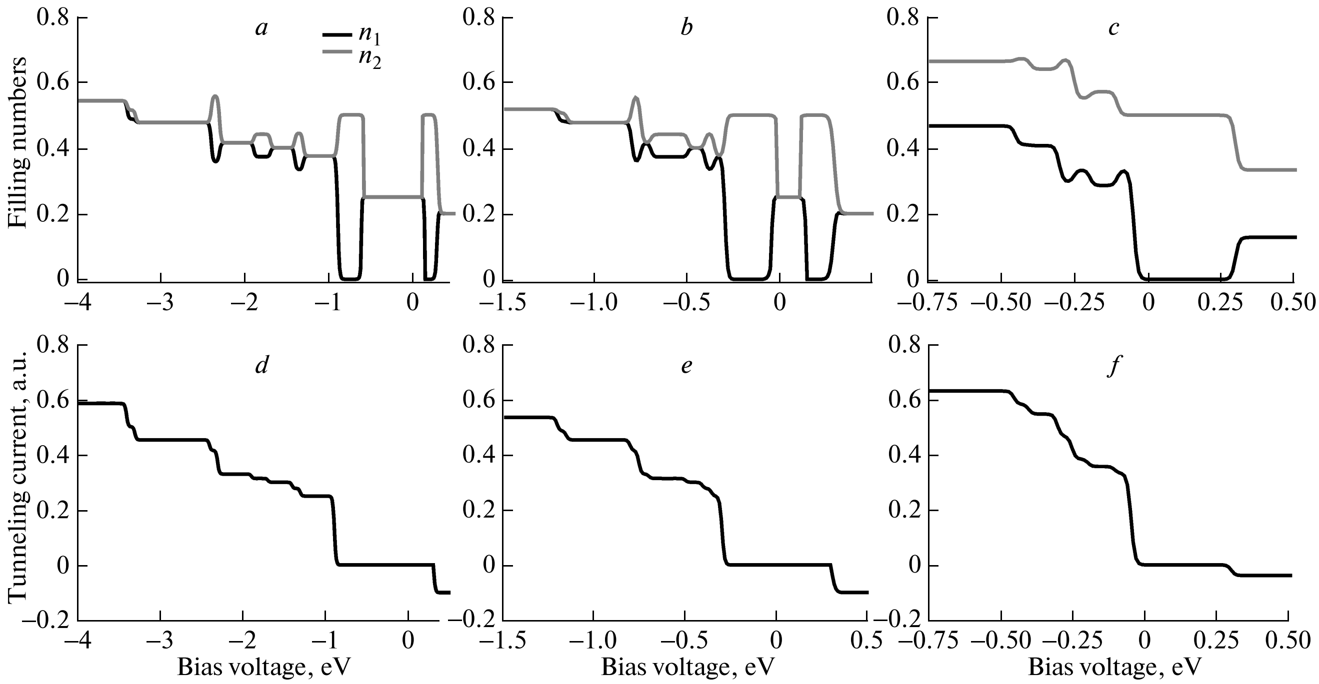

Fig. 6. Two-level system filling numbers (a–c) and tunneling current (d–f) as functions of the applied bias voltage in the case where both energy levels are located below the sample Fermi level. The parameters $\epsilon_1 = -0.1$, $\epsilon_2 = -0.3$, $\Gamma_{k1} = \Gamma_{k2} = 0.01$, $\Gamma_{p1} = \Gamma_{p2} = 0.01$ are the same for all the figures; $U_{12} = 1.0$, $U_{11} = 1.5$, $U_{22} = 1.6$ (a,d); $U_{12} = 0.4$, $U_{11} = 0.5$, $U_{22} = 0.65$ (b,e); $U_{12} = 0.15$, $U_{11} = 0.25$, $U_{22} = 0.4$ (c,f)

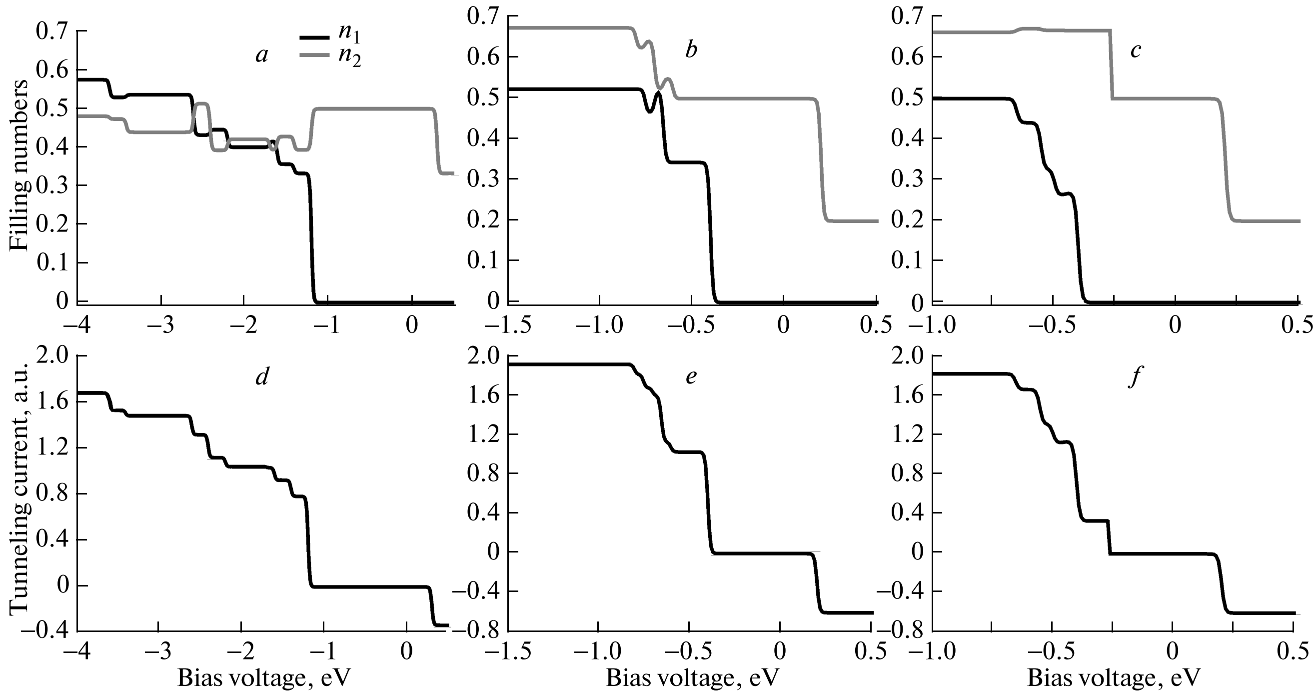

Fig. 7. Two-level system filling numbers (a–c) and tunneling current (d–f) as functions of the applied bias voltage in the case where one energy level is located above and the other — below the sample Fermi level. The parameters $\epsilon_1 = 0.2$, $\epsilon_2 = -0.3$, $\Gamma_{k1} = \Gamma_{k2} = 0.01$, $\Gamma_{p1} = \Gamma_{p2} = 0.01$ are the same for all the figures; $U_{12} = 1.0$, $U_{11} = 1.4$, $U_{22} = 1.7$ (a,d); $U_{12} = 0.1$, $U_{11} = 0.25$, $U_{22} = 0.8$ (b,e); $U_{12} = 0.1$, $U_{11} = 0.15$, $U_{22} = 0.25$ (c,f)

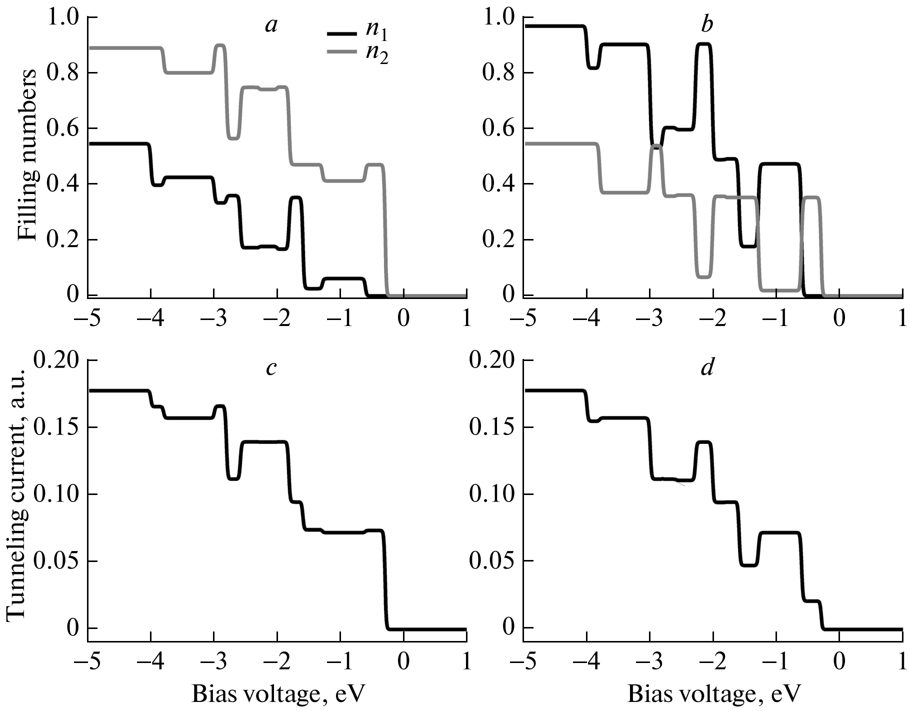

Fig. 8. Two-level system filling numbers (a,b) and tunneling current (c,d) as functions of the applied bias voltage in the case where both energy levels are located above the sample Fermi level for different values of tunneling rates. The parameters $\epsilon_1 = 0.6$, $\epsilon_2 = 0.3$, $U_{12} = 1.0$, $U_{11} = 1.5$, $U_{22} = 1.6$ are the same for all the figures; $\Gamma_{k1} = 0.06$, $\Gamma_{p1} = 0.05$, $\Gamma_{k2} = 0.15$, $\Gamma_{p2} = 0.005$ (a,c); $\Gamma_{k1} = 0.15$, $\Gamma_{p1} = 0.005$, $\Gamma_{k2} = 0.06$, $\Gamma_{p2} = 0.05$ (b,d)

case, an interplay between "single electron" nonequilibrium occupation effects and Coulomb correlation effects exists and at a certain bias charge, the redistribution is accompanied by negative differential conductivity.

The case of both energy levels located above the sample Fermi level is shown in Fig. 8. If the tunneling transfer rate from the sample to the lower energy level is the largest in the system and the tunneling transfer amplitude from the lower energy level to the tip is the lowest (Fig. 8a,c), we see that the local charge in the system is mostly accumulated on the lower energy level. Vice versa, if the tunneling transfer rate from the sample to the upper energy level is the largest and the one from the upper energy level to the tip is the lowest in the system (Fig. 8b,d), then the local charge is mainly accumulated on the upper energy level and consequently inverse occupation occurs. But due to the Coulomb interaction, three ranges of the applied bias exist where local charge is mostly localized on the lower energy level $\varepsilon_2 < eV < \varepsilon_1$, $\varepsilon_2 + U_{12} < eV < \varepsilon_1 + U_{12}$, and $\varepsilon_2 + U_{22} + U_{12} < eV < \varepsilon_1 + U_{11} + U_{12}$.

Inverse occupation also occurs when energy levels are located on the opposite sides of the sample Fermi level (Fig. 9a) or when both energy levels are below the Fermi level (Fig. 9b). In any case, Coulomb interaction modifies the single-electron occupation behavior, changing with the applied bias from normal occupation to the inverse one or vice versa.

In Fig. 9a, we see several ranges of the applied bias where the charge is distributed differently. These intervals depend on Coulomb interaction values: the entire charge is accumulated on the lower energy level ($n_1 = 0$) for $eV < \varepsilon_1 + U_{12}$; inverse occupation exists (local charge is mostly localized on the upper energy level) for $\varepsilon_1 + U_{12} < eV < \varepsilon_2 + U_{22} + U_{12}$ and $\varepsilon_1 + U_{11} + U_{12} < eV$; charge is equally accumulated on both electron levels, $n_1 = n_2$, if $\varepsilon_2 + U_{22} + U_{12} < eV < \varepsilon_1 + U_{11} + U_{12}$.

If both energy levels are located below the Fermi level (Fig. 9b), there are similar applied bias ranges in which charge is distributed differently (equally for $\varepsilon_1 < eV < \varepsilon_2 + U_{12}$, inversely if $\varepsilon_1 + U_{12} < eV < \varepsilon_2 + U_{22} + U_{12}$ and $\varepsilon_1 + U_{11} + U_{12} < eV$, and so on).

The appearance of negative conductivity regions is the most essential feature of the tunneling characteristics, depicted in Figs. 8c,d and 9c,d. We stress once

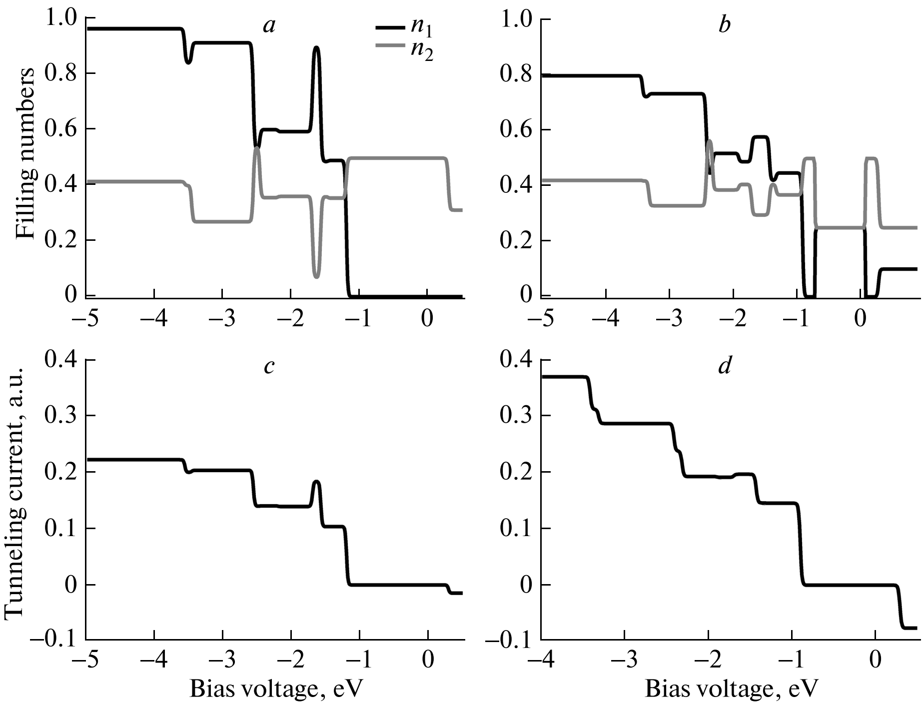

Fig. 9. Two-level system filling numbers (a,b) and tunneling current (c,d) as functions of the applied bias voltage in cases where one energy level is located above and the other — below (a,c) and both energy levels are located below (b,d) the sample Fermi level for different values of tunneling rates. The parameters $\Gamma_{k1} = 0.15$, $\Gamma_{p1} = 0.005$, $\Gamma_{k2} = 0.06$, $\Gamma_{p2} = 0.05$ are the same for all the figures; $\epsilon_1 = 0.2$, $\epsilon_2 = -0.3$, $U_{12} = 1.0$, $U_{11} = 1.4$, $U_{22} = 1.7$ (a,c); $\epsilon_1 = -0.1$, $\epsilon_2 = -0.3$, $U_{12} = 1.0$, $U_{11} = 1.5$, $U_{22} = 1.6$ (b,d)

more that the formation of negative conductivity is an interplay between nonequilibrium effects connected with the tunneling current and Coulomb correlations.

Recently, the perturbative approach was used to investigate a similar system coupled to magnetic leads [18]. The authors obtained staircase tunneling characteristics connected with many-particle states in the first nonvanishing order $\propto \Gamma_k \Gamma_p$. The developed perturbation theory over the equilibrium of the quantum dot does not take nonequilibrium effects connected with the tunneling current into account. Nonequilibrium filling numbers like $n_T(\varepsilon_i)$ do not therefore appear and consequently effects such as the inverse occupation of states in the quantum dots and negative tunneling conductivity are absent in the theory suggested in [18].

4. CONCLUSION

We investigated tunneling through the two-level system with strong Coulomb interaction between localized electrons taking all-order correlators of local electron density into account. It was shown that charge redistribution between electron states is strongly governed by the Coulomb correlations and is of reentrant type. The dependence of electron filling numbers on applied bias is quite different from that for noninteracting electrons. The existence of charge redistribution effects means that adjusting the applied bias allows controling spatial redistribution of localized charges. Diverse possibilities for local charge accumulation and charge switching therefore exist for such systems.

In addition, at certain values of the Coulomb interaction of localized electrons, we can obtain a correlation-induced inverse occupation of the two-level system in different ranges of the applied bias. Inverse occupation is mostly pronounced in asymmetric contacts with different tunneling rates to the sample and to the lead, and when one energy level lies below and another above the Fermi level.

By changing the tunneling contact parameters (tunneling rates of each level to the leads), we can observe an interplay between two mechanisms responsible for non-equilibrium occupation of each level: inverse occupation induced by the tunneling current of a two-level system at a particular ratio between tunneling rates (which exists in the absence of Coulomb interaction) and inverse occupation connected only with Coulomb interaction of localized electrons.

We revealed that for some parameter range, the system demonstrates negative tunneling conductivity in certain ranges of the applied bias voltage. A negative tunneling conductivity is revealed in the asymmetric case $\Gamma_{ki} \neq \Gamma_{pi}$ (Figs. 8 and 9) and is more pronounced if both energy levels are located above the Fermi level. When energy levels are located on the opposite sites of the Fermi level, the negative tunneling conductivity is much weaker and when both of them are positioned below the Fermi level, it is negligible.

The financial support by the RFBR, grant №11-02-00317_a, Leading Scientific School grant №4375.2012.2, and rasprogram ofn II.3.

REFERENCES

1. M. V. Feigel'man and A. S. Ioselevich, Pis'ma v Zh. Eksp. Teor. Fiz. **81**, 341 (2005).
2. I. S. Beloborodov, A. V. Lopatin, V. M. Vinokur, and K. B. Efetov, Rev. Mod. Phys. **79**, 469 (2007).
3. J. Konig and Y. Gefen, Phys. Rev. B **71**, 201308(R) (2005).
4. A. Levi Yeyati and M. Buttiker, Phys. Rev. B **62**, 7307 (2000).
5. P. Pou, R. Perez, F. Flores et al., Phys. Rev. B **62**, 4309 (2000).
6. J. Kondo, Progr. Theor. Phys. **32**, 37 (1964).
7. Y. Goldin and Y. Avishai, Phys. Rev. B **61**, 16750 (2000).
8. A.-P. Jauho, N. Wingreen, and Y. Meir, Phys. Rev. B **50**, 5528 (1994).
9. J. Konig, T. Pohjola, H. Schoeller, and G. Schon, Physica E **6**, 371 (2000).
10. Y. Meir, N. S. Wingreen, and P. Lee, Phys. Rev. Lett. **66**, 3048 (1991).
11. D. V. Averin, A. N. Korotkov, and K. K. Likharev, Phys. Rev. B **44**, 6191 (1991).
12. I. M. Ruzin, V. Chandrasekhar, E. Levin, and L. Glazman, Phys. Rev. B **45**, 13469 (1992).
13. K. Kikoin and Y. Avishai, Phys. Rev. Lett. **86**, 2090 (2001).
14. L. V. Keldysh, Sov. Phys. JETP **20**, 1018 (1964).
15. P. I. Arseyev, N. S. Maslova, V. I. Panov, and S. V. Savinov, Zh. Eksp. Teor. Fiz. **121**, 225 (2002).
16. N. S. Maslova, Pis'ma v Zh. Eksp. Teor. Fiz. **51**, 627 (1990).
17. V. V. Kuznetsov, A. K. Savchenko, D. R. Mace et al., Phys. Rev. B **56**, R15533 (1997).
18. A. U. Sharfutdinov and I. S. Burmistrov, arXiv: 1103.2425v1.